

# Global Sensitivity Analysis for a Comprehensive Char Conversion Model in Oxy-fuel Conditions

Troy Holland and Thomas H. Fletcher\*

350 CB, Chemical Engineering Department, Brigham Young University, Provo, Utah 84602, United States

**ABSTRACT:** Oxy-fired coal combustion is a promising potential carbon capture technology. Predictive CFD simulations are valuable tools in evaluating and deploying oxy-fuel and other carbon capture technologies either as retrofit technologies or for new construction. However, accurate predictive simulations require physically realistic submodels with low computational requirements. In particular, comprehensive char oxidation and gasification models have been developed that describe multiple reaction and diffusion processes. This work focuses on the sensitivity of a recent comprehensive char conversion code named CCK, which treats surface oxidation and gasification reactions as well as the processes such as film diffusion, pore diffusion, ash encapsulation, and annealing. In this work the CCK code was adapted for the conditions of an oxy-coal system and subjected to global sensitivity analysis techniques in an effort to rank fundamental input parameters in order of importance. Comprehensive char conversion codes have dozens of fundamental parameters, some of which are not well-defined. Global sensitivity analysis was used to identify the most important submodels in order to direct additional research on model improvement. Results of this analysis showed that the annealing model, the oxidation reaction order, the swelling model, and the mode of burning parameter are the most influential and therefore prime candidates for improvement.

## 1. INTRODUCTION

Coal-fired power plants have provided a substantial percentage of global electricity for decades, and current outlooks indicate that they will continue to do so for the foreseeable future. The high proportion of electrical power generation is matched by a correspondingly high proportion of CO<sub>2</sub> emissions. In order to meet regulatory targets for reduced emissions, carbon capture and sequestration techniques must be employed, and oxy-coal combustion is a promising potential solution.

Oxy-coal combustion has been reviewed thoroughly elsewhere,<sup>1,2</sup> but in essence it consists of injecting high-purity O<sub>2</sub> with the pulverized coal rather than the conventional air-fired method. To reduce the boiler temperatures to manageable levels, the flue gas is typically recycled, producing a combustion environment with high concentrations of CO<sub>2</sub>, O<sub>2</sub>, and (potentially) H<sub>2</sub>O. The flue gas then contains very high concentrations of CO<sub>2</sub>, and the CO<sub>2</sub> is thus relatively easy to capture.

While this system simplifies carbon capture, it also radically changes the environment the coal particles experience. The new environment changes the O<sub>2</sub> diffusion rate, may cool the char particle via endothermic gasification, and may alter the overall char consumption rate due to gasification reactions.<sup>3</sup> These effects and others such as reduced flame temperature, delayed ignition, decreased acid gases, and increased gas emissivity can largely be ascribed to differences between CO<sub>2</sub> and N<sub>2</sub> (the respective diluents in oxy-coal and air-fired pulverized coal systems).<sup>1</sup> The change in diluent gas induces several interrelated effects that alter the burnout time and radiative behavior of the system, so accurate CFD predictions of oxy-coal combustion require models that describe these phenomena. This work supports CFD modeling of oxy-coal boilers either for the retrofit of existing boilers or the construction of new oxy-coal-fired power plants by identifying the most sensitive submodels in comprehensive char oxidation codes. Specifically,

the parameter sensitivity of the carbon conversion kinetics (CCK) code<sup>4,5</sup> was examined for oxy-coal conditions. The CCK char combustion code was chosen since it contains a high degree of physical detail in several submodels for char conversion via CO<sub>2</sub>, H<sub>2</sub>O, and O<sub>2</sub> gasification. A sensitivity analysis on this code was used to identify the most influential submodels in oxy-fuel conditions, which can in turn guide future research and submodel improvements.

## 2. EXPERIMENTAL SECTION

To conduct a relevant sensitivity analysis, the model was run at conditions related to real-world application. Here, the most applicable conditions are the oxy-coal combustion environment, so experimental data from the literature were chosen as a reference point at useful conditions. The experimental data also allowed the kinetic parameters to be optimally fit and fixed, so that the subsequent sensitivity analysis is most relevant at oxy-coal conditions with the kinetics of the specific coals in question, though the results are believed to be broadly applicable. The experimental data referenced here were collected by Shaddix and Molina<sup>6</sup> and Geier et al.<sup>7</sup> The reactor consists of a burner-stabilized flat flame, a quartz chimney for gas and particles to flow through, and a coal particle inlet in the center of the burner. The coal particle flow rate was sufficiently low that particles did not affect each other or the bulk gas composition. The data were for two subbituminous coals (Black Thunder and North Antelope) and two high-volatile bituminous coals (Utah Skyline and Pittsburgh seam) which were subjected to conditions of 14 or 16% H<sub>2</sub>O, 12, 24, or 36% O<sub>2</sub>, and the balance CO<sub>2</sub>, at gas temperatures ranging from approximately 1400 to 1700 K. The proximate and ultimate analyses of the coals and a summary of experimental conditions are given in Tables 1 and 2. The char particles were in the reactor for up to approximately 0.1 s (post-devolatilization), and on the order of 1,000 particle temperature and diameter data points were collected for each

Received: August 30, 2016

Revised: October 3, 2016

Published: October 4, 2016



Table 1. Proximate and Ultimate Analysis of Coal Particles between 73 and 105  $\mu\text{m}$ 

coal	moisture (% AR)	ash (% AR)	volatiles (% AR)	C (% daf)	H (% daf)	O (% daf) <sup>a</sup>	N (% daf)	S (% daf)
Black Thunder	9.34	4.84	42.34	68.96	5.00	25.41	0.97	0.45
Utah Skyline	1.69	10.2	40.79	79.4	6.09	12.25	1.67	0.59
Pittsburgh	0.47	6.95	35.89	81.26	5.55	10.17	1.54	2.16
North Antelope	10.83	5.54	39.64	72.12	5.45	21.08	1.00	0.35

<sup>a</sup>By difference.Table 2. Summary of Experiments for Coal Particles between 53 and 125  $\mu\text{m}$ 

coal	O <sub>2</sub> (mol %)	CO <sub>2</sub> (mol %)	H <sub>2</sub> O (mol %)	peak particle temp (K)	peak gas temp (K)
Black Thunder	12	74	14	1732	1741
	24	62	14	1919	1710
	36	50	14	2147	1726
Pittsburgh	12	74	14	1889	1741
	24	62	14	2077	1710
	36	50	14	2248	1726
Utah Skyline	12	72	16	1954	1697
	24	60	16	2181	1700
	36	48	16	2564	1714
North Antelope	12	72	16	1931	1697
	24	60	16	2108	1700
	36	48	16	2414	1714

condition. The data collected included particle temperature and particle diameter.

### 3. CHAR CONVERSION MODELING

Several char conversion models include complex submodels that attempt to capture the most important chemistry and transport effects of char conversion. The code used here is an extension of the CCK code<sup>4,5</sup> with minor adjustments to make the code functional in the extremes of oxy-coal combustion. These modifications include a more stable temperature solver with informed initial guess values that result in rapid convergence times, step-size independence, and successful model execution at extremely high temperature (appropriate for highly elevated O<sub>2</sub> concentrations) or high H<sub>2</sub>O and CO<sub>2</sub> concentration environments. Predecessors of this code include carbon burnout kinetics—extended (CBK/E<sup>8</sup>) and carbon burnout kinetics—gasification (CBK/G)<sup>9</sup> codes (which grew out of the carbon burnout kinetics or CBK code<sup>10</sup>). Like other recent CBK iterations, CCK includes the kinetic mechanism shown in eqs R1–R8 to model the oxidation and gasification of carbon. Note that in this mechanism the C(O) complexes in reactions R3, R5, and R7 represent distinct species with separate reactant pools, as indicated by their subscripts. This means that conversions via O<sub>2</sub>, CO<sub>2</sub>, and H<sub>2</sub>O all have different pathways and do not share the same C(O) complex pools as a common reactant (i.e., if reaction R1 were to be very rapid and produce a high concentration of the C(O) <sub>$\alpha$</sub>  complex, this complex would not facilitate reaction R5 or R7, nor hinder reaction R4 or R6). This reaction formulation is in accordance with section 3.2 of Liu and Niksa.<sup>9</sup> The CCK code also includes the other models shown in Table 3.

The extended CCK code contains over 300 input parameters that include effects such as reaction kinetics, pore diffusion, thermal annealing, ash layer buildup, particle size distribution, and distributed activation energies. The object of this study is to statistically determine the most sensitive parameters of this

model in oxy-fuel combustion environments to optimally target further research and model improvement for those parameters. More detailed descriptions of the CCK- and CBK-type models are available elsewhere.<sup>4,5,8–10</sup>

### 4. SENSITIVITY ANALYSIS METHOD

The primary focus of this work is the sensitivity analysis, including the methods and results. Sensitivity can be measured in many ways by such standards as output variance, absolute change in output, and correlation of model inputs with model outputs, etc. These measures do not necessarily give the exact same information, but they reveal, broadly, which input variables have the greatest impact on model output quantities of interest. In the analyses presented here, three methods were employed. The first is a simple correlation check, the second considers the magnitude of the change in the outputs induced by the change in the inputs, and the third examines the monotonicity of input/output relationships. The three methods were chosen because they could be applied with reasonable coding and computational effort (once the codes were written and validated, they consumed approximately 1 week of computational time crudely parallelized on a Mac Pro, 2014 model) and yielded results at an adequate level of detail (i.e., the results of the sensitivity analysis were consistent between computational runs).

These three methods were applied by varying all parameters simultaneously, followed by a comparison of the input and output matrices. Depending on the comparison method, the sensitivity test assumed either linear or monotonic variation of inputs with outputs. The test also assumed that any given variable would induce roughly the same order of magnitude change in the outputs. These assumptions are not rigorously true, but the results presented below show they are adequate to rank the various submodels and parameters in order of importance. Also, it must be emphasized that the linearity assumption is far more valid than might initially be supposed. In this case, the values of the parameters are known, and each parameter is associated with a linear coefficient that can be determined via multiple linear regression. The regressed model remains linear as long as the coefficients do not have a multiplicative, exponential, or logarithmic relationship to each other. This is valid regardless of the fact that the parameter, when employed in the CCK model, can (and often does) undergo any number of nonlinear operations or transformations.

The sensitivity analysis is of general interest because some of the parameters used in comprehensive char conversion models may be used more as fitting parameters rather than measurable, physical quantities.<sup>6,13</sup> Such fitting parameters weaken the predictive capability of the model. For example, physical measurements of tortuosity are generally unavailable, so relevant parameters are often tuned to specific data sets. The CCK model includes several submodels with numerous parameters, many of which have second order and higher

Table 3. CCK Submodels

submodel name	model form
particle energy balance	$m_p C_p \frac{dT_p}{dt} = h A_p (T_g - T_p) + \sigma \epsilon_p A_p (T_s^4 - T_p^4) + \sum_i r_{p,i} \Delta H_{rxn,i} \quad (1)$
surface reactions <sup>5</sup>	$2C + O_2 \rightarrow C(O)_\alpha + CO \quad (R1)$ $C + O_2 + C(O)_\alpha \rightarrow C(O)_\alpha + CO_2 \quad (R2)$ $C(O)_\alpha \rightarrow CO \quad (R3)$ $CO_2 + C \leftrightarrow C(O)_\beta + CO \quad (R4)$ $C(O)_\beta \rightarrow CO \quad (R5)$ $C + H_2O \leftrightarrow C(O)_\gamma + H_2 \quad (R6)$ $C(O)_\gamma \rightarrow CO \quad (R7)$ $C + 2H_2 \rightarrow CH_4 \quad (R8)$
Langmuir–Hinshelwood-type Reactions <sup>5</sup>	$R_{C-O_2} = \frac{k_1 k_2 P_{O_2}^{(1+n_1)} + k_1 k_3 P_{O_2}}{k_1 P_{O_2} + \frac{k_3}{2}} \quad (2)$ $R_{C-CO_2} = \frac{k_4 P_{CO_2}}{1 + \frac{k_4}{k_5} P_{CO_2} + \frac{k_{4r}}{k_5} P_{CO} + \frac{k_6}{k_7} P_{H_2O} + \frac{k_{6r}}{k_7} P_{H_2}} \quad (3)$ $R_{C-H_2O} = \frac{k_8 P_{H_2O}}{1 + \frac{k_4}{k_5} P_{CO_2} + \frac{k_{4r}}{k_5} P_{CO} + \frac{k_6}{k_7} P_{H_2O} + \frac{k_{6r}}{k_7} P_{H_2}} \quad (4)$
thermal annealing <sup>10</sup>	$\frac{dN_i}{dt} = -N_i A_i \exp\left(\frac{E_A}{RT_p}\right) \quad (5)$
Thiele modulus	$\phi_j = \frac{d_p}{2} \sqrt{\frac{\rho_c v_j (n_j + 1) R_{j,s}}{2 D_{eff,j} C_{j,s}}} \quad (6)$
effectiveness factor	$\eta_j = \frac{1}{\phi_j} \left[ \coth\left(3\phi_j - \frac{1}{3\phi_j}\right) \right] \quad (7)$
multicomponent diffusion	$D_{i,mix} = \frac{1 - y_i}{\sum_{j=1, j \neq i}^{species} \frac{y_j}{D_{i,j}}} \quad (8)$
random pore model <sup>11</sup>	$\frac{A_p}{A_{p,0}} = (1 - x) \sqrt[2]{1 - \psi \ln(1 - x)} \quad (9)$
particle swelling <sup>8</sup>	$\frac{d}{d_0} = 8.67 - 0.0833 X_C \quad \text{if } 89 \leq X_C \leq 92 \quad (10)$ $\frac{d}{d_0} = -0.0458 + 0.01459 X_C \quad \text{if } 72 \leq X_C \leq 89 \quad (11)$ $\frac{d}{d_0} = 1 \quad \text{if } X_C < 72 \quad (12)$
CO/CO <sub>2</sub> ratio <sup>12</sup>	$\frac{CO}{CO_2} = A_C \exp\left(\frac{E_C}{RT_p}\right) \quad (13)$

interactive relationships. A sensitivity analysis was therefore performed to rank the parameters in order of importance. Because of the many complex interactions between model parameters, the sensitivity analysis was global, over the entire range of physically reasonable parameter space, and with all parameters of interest varying simultaneously. This is the first time such a formal global analysis has been applied to a comprehensive char conversion code. The results of this analysis identified prime candidates for model improvement, and these candidates generally have an equivalent submodel or parameter in other comprehensive char conversion codes,

which allows the results shown here to apply broadly to conceptually similar codes.

#### 4.1. Determination of the Fundamental Parameters.

As a first step, the set of model parameters was reduced to fundamental parameters, defined as those that were not computed from other parameters. This reduced the number of parameters to approximately 50, and these were further reduced to 36 parameters by testing only the physically feasible range of the combined activation energies ( $E$ ) and preexponential factors ( $A$ ) for the relevant chemical kinetics. Allowing both  $E$  and  $A$  to vary freely and independently of each other would result in many cases where the reaction in question

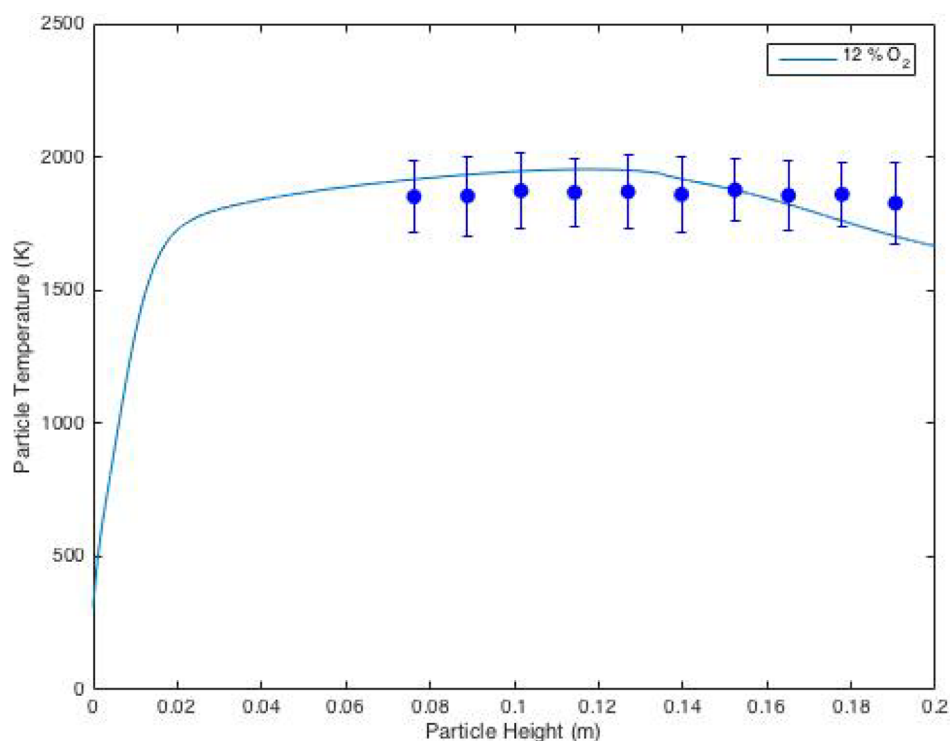


**Figure 1.** Predicted (lines) and measured (points) particle temperatures of  $90\ \mu\text{m}$  initial char diameter North Antelope coal particles in 12%  $\text{O}_2$ . The error bars represent the spread of approximately 95% of the data. Data are from Greier et al.<sup>7</sup>

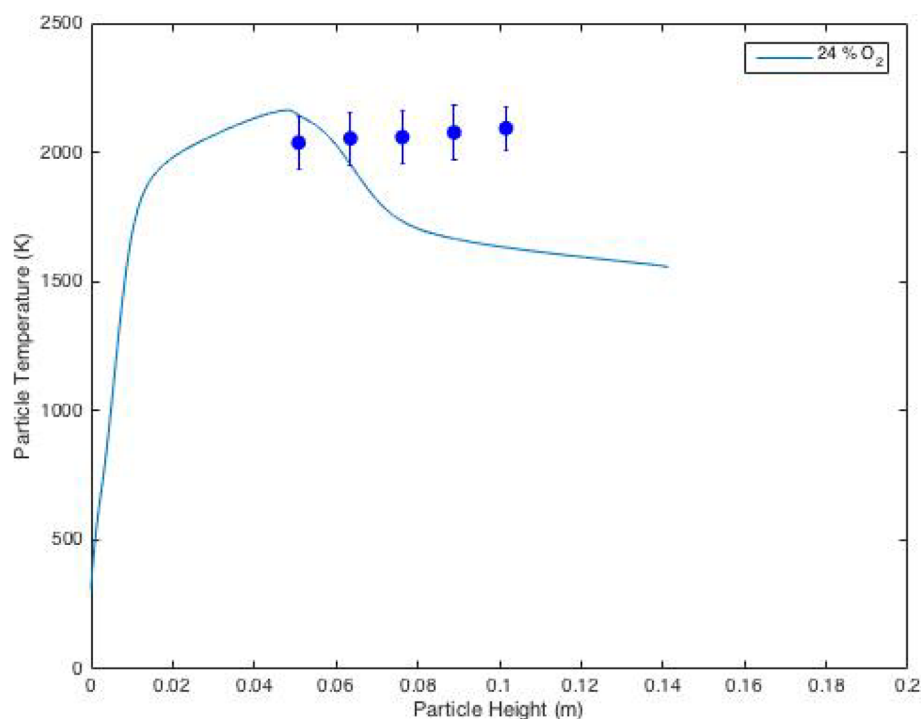


**Figure 2.** Predicted (lines) and measured (points) particle temperatures of  $90\ \mu\text{m}$  initial char diameter North Antelope coal particles in 24%  $\text{O}_2$ . The error bars represent the spread of approximately 95% of the data. Data are from Greier et al.<sup>7</sup>

essentially did not occur, and many others where it occurred orders of magnitude too rapidly, rendering the analysis physically meaningless. Choosing a value for the first parameter in any set of correlated parameters reduces the physically reasonable range of the other parameters, but this effect is particularly import in the case of the Arrhenius form kinetics.

The exponential form found in Arrhenius kinetics is a specific example of a mathematical form common even outside of kinetic systems and is shown in eq 14. In general, the exponential term changes rapidly with small changes in the exponential parameter “ $b$ ”, but “ $y$ ” is relatively tightly constrained, which in turn sharply prescribes acceptable values

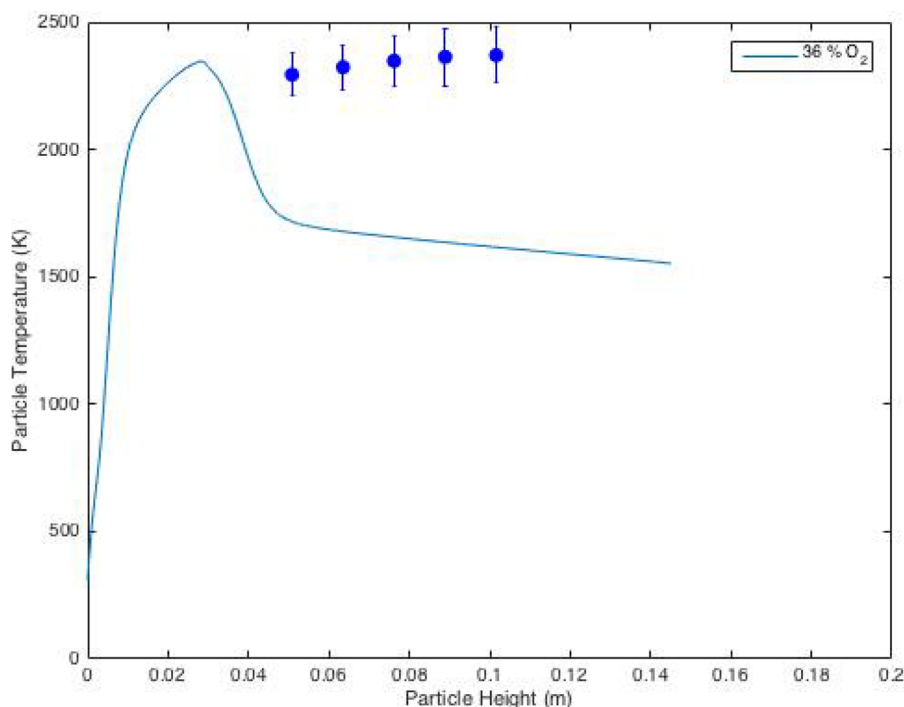


**Figure 3.** Predicted (lines) and measured (points) particle temperatures of 90  $\mu\text{m}$  initial char diameter North Antelope coal particles in 36%  $\text{O}_2$ . The error bars represent the spread of approximately 95% of the data. Data are from Greier et al.<sup>7</sup>

of “ $a$ ” once  $b$  is chosen. This complicates sensitivity analyses because often it is unknown exactly which bounds  $y$  should have, as is the case in this system of eight reaction equations interrelated by Langmuir–Hinshelwood-type kinetics.

$$y = a \exp(b) \quad (14)$$

However, the analysis can still be executed in a useful manner. Because the analysis seeks to determine the importance of a given reaction pathway (not the importance of  $A$  or  $E$  individually), reducing kinetic parameters to one parameter per reaction does not limit the usefulness of the sensitivity analysis. Instead, the one free parameter is allowed a sufficient range to express all feasible values of  $y$  without allowing any physically meaningless pairs of  $a$  and  $b$  (or in the specific case of kinetics,  $A$  and  $E$ ). The analysis in fact indicated that the most important parameters were often kinetic parameters. This is to be expected and served as a useful final check of the analysis codes, but does not offer much in the way of new insight, so the kinetic parameters were optimized and fixed at stationary values. The kinetic parameters were therefore excluded from the sensitivity analysis, which is desirable because while these kinetic parameters are highly sensitive, reliable, general correlations for coal oxidation and gasification kinetic parameters do not exist. Therefore, a precise, predictive code must fit the kinetic parameters using data relevant to the specific combustion scenario. The kinetic parameters for the surface reaction resulting from this curve fit were held constant for the subsequent sensitivity analyses, reducing the number of parameters to 27. Note that the optimized kinetic parameters are not a unique solution (as is typically the case of all but the simplest optimizations) and that different nominal values of the fundamental parameters could shift the optimized kinetic values. However, no reasonable nominal values would significantly reduce the sensitivity of the kinetic parameters, and no reasonable values of the kinetic

parameters would result in a radically different sensitivity analysis.

Also note that the word “fit” here does not imply the simple linearization of a global equation that results in a slope and intercept that correspond to values of the activation energy and preexponential factor. Because of the great complexity of the model, the fit was obtained by fixing all parameter values except for the kinetic parameters of eqs R3 and R7, and using MATLAB `fmincon` optimization software to minimize the error between the data and the model prediction, where the data were divided into particle size “bins” to minimize the error introduced by a range of particle sizes. All other kinetic parameters are directly related to the values of the parameters of eqs R3 and R7, as in the other most recent iterations of CBK-type codes.<sup>5,8,9</sup> Examples of the fit of particle temperature data during char conversion in an oxy-fuel environment are shown in Figures 1–3. Table 4 shows the optimized kinetic parameters.

Also note that the error bars in Figures 1–3 show two standard deviations from the mean; while the error bars are quite wide, this is a result a significant particle-to-particle variation rather than actual measurement error. That is, the particles vary substantially in diameter and ash content (and

**Table 4.** Optimized Kinetic Parameters.<sup>a</sup>

coal type	$E_{A,7}$ (kJ/mol)	$E_{A,3}$ (kJ/mol)	$A_7$ ( $\text{s}^{-1}$ )	$A_3$ (unitless)
Black Thunder	239	151	$1.00 \times 10^{11}$	$6.64 \times 10^8$
North Antelope	248	152	$1.75 \times 10^{11}$	$3.62 \times 10^9$
Utah Skyline	230	156	$5.00 \times 10^{11}$	$2.42 \times 10^{11}$
Pittsburgh	259	161	$1.16 \times 10^{11}$	$6.64 \times 10^8$

<sup>a</sup>Note that because  $E$ 's and  $A$ 's are strongly correlated, these are only one of several sets of possible values where a larger (or smaller)  $E_A$  may be compensated for by a larger (or smaller)  $A$  value.

Table 5. Parameters of the Sensitivity Analysis

parameter	description	min	max	nominal
$V_{ASTM}$	ASTM volatiles; well-known for common coals <sup>a</sup>	−1%	+1%	various
$x_{ash}$	Ash (dry basis); well-known for common coals <sup>a</sup>	−1%	+1%	various
$x_C$	C (daf); well-known for common coals <sup>a</sup>	−1%	+1%	various
$x_H$	H (daf); well-known for common coals <sup>a</sup>	−1%	+1%	various
$D_{P0}$	initial raw coal diameter (used mean value of a known size cut, and sufficient variation to capture the bulk of the size spread) <sup>b</sup>	−20%	+20%	various
$E_A$	mean activation energy of char annealing from CBK (kcal/mol), with ranges chosen from the scatter in the data <sup>10</sup>	5.0	40	16.4
$E_C$	activation energy in the CO/CO <sub>2</sub> production ratio model; wide uncertainty from CBK 8 (cal/mol) <sup>12b</sup>	−50%	+50%	9,000
$d_{grain}$	size of ash grains in the char particle (micrometers); <sup>5,10</sup> bounds exceptionally wide because the parameter is thought to be relatively unimportant and extreme cases test that theory	0.1	10	5
$V_{HT}$	high-temperature volatile release	$1.1V_{ASTM}$	$1.3V_{ASTM}$	$1.2V_{ASTM}$
$n_1$	oxidation reaction order; <sup>9</sup> wide variation in data for this parameter, so entire range allowed	0	1	1
$P$	pressure of the combustion system (atm); CCK code most suited for roughly atmospheric pressure experiments	0.9	1.1	1
$\phi_{af}$	ash–film porosity <sup>10</sup>	0	0.5	0.17
$t_r$	char particle residence time (s); case specific and largely of interest to observe the sensitivity of late burn out to the uncertainty in short residence times	various	various	various
$T_{P0}$	initial coal particle temperature (K); room temperature values for raw coal and about 1300 K for cases when the model is initiated post-devolatilization	300	1500	300
$\alpha$	mode of burning parameter; various conditions spannable across entire range of the mode of burning. $\frac{\rho}{\rho_0} = \left(\frac{m}{m_0}\right)^\alpha$	0	1	various
$\lambda_a$	thermal conductivity of the ash (cal/(cm <sup>a</sup> s <sup>a</sup> K)); value likely unimportant so extreme range used to test this theory	0.001	0.01	0.005
$\psi$	random pore model parameter <sup>19</sup> $\frac{S}{S_0} = (1 - X)\sqrt{(1 - \psi \ln(1 - X))}$	1	19	4.6
$\rho_a$	density of the ash (gm/cm <sup>3</sup> )	2	3	2.65
$\rho_c$	density of the coal (gm/cm <sup>3</sup> )	1.2	1.4	1.3
$\sigma_{E_A}$	standard deviation of the activation energy distribution for char annealing (kcal/mol) <sup>10</sup>	1.5	1.65	1.58
$\tau/f$	random pore model tortuosity parameter <sup>5</sup>	1	24	12
$d/d_0$	particle swelling (diameter/initial particle diameter)	0.9	1.1	various

<sup>a</sup>Absolute percent. <sup>b</sup>Relative percent.

therefore combustion temperature), so the standard deviation bars actually show the range of roughly 95% of the data, rather than actual measurement error, which is on the order of 20 K. The single, solid line is for one particle size and one ash fraction, while the error bars show the range of prediction curves expected for the entire range of ash content and particle sizes. The model fit to the data is (in high-O<sub>2</sub> cases) quite poor, and the data do not show late-stage particle cooling as would be expected. The inadequate fit is partially due to particle-to-particle variation but mostly a result of inadequate treatment of oxy-fuel conditions by the model, and a potential skew introduced by the data collection system (particles that are too small or too cool are not detectable in this system). Similarly, the late-stage burnout particles are likely not observed because they have cooled below the detection threshold. Because the CCK code was not originally intended for oxy-coal conditions, it is unsurprising that the submodels are not entirely appropriate; the main purpose of this work is in fact to highlight the submodels most in need of improvement. Figure 1 shows a very acceptable fit within the range of data (as might be expected with a more conventional O<sub>2</sub> concentration), while predictions in Figures 2 and 3 do not agree well with the data, indicating the need for substantial model changes in typical oxy-coal conditions.

**4.2. Determination of Parameter Ranges.** The next step of the analysis was to determine simulation input values for each parameter, along with a range of permissible values. The range of permissible values was used to set up a Latin

hypercube sampling scheme. The hypercube accepts as inputs the allowed range and probability distribution of each parameter. The range is then divided into a specified number of equiprobable intervals, and one value of the parameter is chosen randomly from each interval. For example, if 10 intervals were chosen, the parameter space would be divided into 10 pieces. In the case of a uniform probability distribution, each of these 10 parameters would be of equal “length” in parameter space, while in the case of a normal distribution, the intervals very near the mean value would be quite short in terms of parameter space and the intervals in the tail would be extremely long. Because each interval has a single value sampled from it, most of the samples would cluster around the mean, and the low-probability sample space would be relatively sparsely covered. This process is repeated for each parameter, and the values are then randomly paired.<sup>14</sup> The result is a matrix in which each column contains randomly ordered, unbiased, space-filling samples from the range of some parameter, and each row is a complete set of all necessary input parameters for a single computational experiment. The number of columns equals the number of parameters, and the number of rows equals the number of specified intervals, and is the number of computational experiments to be performed. Thus, a higher number of rows more carefully explores the parameter space but requires additional computational time that scales linearly with  $n$  (the number of rows in the experimental matrix).

The Latin hypercube design matrix was used to perform 10,000 experiments for 12 different sets of experimental conditions (i.e., four coals and three O<sub>2</sub> conditions). The sensitivity analysis was found to be well-converged at this number of computer experiments. The very large number of parameters to be explored (and their exponentially greater pairwise and higher interactions) made for extremely noisy computational experiments, and 10,000 runs were necessary to clearly and consistently determine the pattern of sensitivity. The results of each set of 10,000 experiments were evaluated using three methods: a simple scatter plot, a partial rank correlation coefficient, and a linear approximation. The scatter plot simply plots the values of a given parameter on the abscissa and the values of the output on the ordinate axis. Because of the large number of parameters, the resultant graphs were, unsurprisingly, entirely obscured by the noise described above, and hence the results are not shown. The other two methods are more robust and yielded satisfactory results, discussed below.

**4.3. Linear Approximation Design.** The modified linear approximation design followed the method described by Frenklach et al.<sup>15</sup> and Box and Draper,<sup>16</sup> adjusted for a Latin hypercube set of experiments. The linear approximation was a global design as described by Saltelli et al.<sup>17,18</sup> with the goal of prioritizing input parameters conducted throughout the entire parameter space of each variable. The linear approximation method calculates an “importance measure” for each parameter, which roughly indicates the rate that a change in input induces a change in output. Here, the importance measure simply means a normalized score that indicates how influential a given parameter is in the model, on a scale from zero to one. The analysis entailed the following steps:

(1) Determine physically reasonable ranges for each parameter. In this case, the ranges were determined from a combination of literature searches and past experience with char burnout. The parameters of interest and their descriptions are given in Table 5 with additional columns to include maximum and minimum allowed values.

(2) Create an  $n \times p$  input matrix  $\mathbf{X}$  of experiments where each column contains the  $n$  input values for one particular variable needed to conduct  $n$  experiments. This was done with the MATLAB `lhsdesign` function to create a Latin hypercube of the parameters as described in section 3.

(3) Execute the model once for each of the  $n$  experiments and store the outputs of interest. Here, the outputs were the total burnout of the particle and the temperature of the particle at each quartile of residence time.

(4) Scale the input matrix  $\mathbf{X}$  values so that they range between  $-1$  and  $1$ . This is accomplished by either linear or logarithmic scaling as appropriate, and is desirable to improve the numerical stability of computations involving large matrices.

(5) Append a column of ones to matrix  $\mathbf{X}$ , which accounts for the free parameter (the intercept) in a system of linear equations and improves the linearized fit.

(6) Solve for the importance measure  $\mathbf{a}$  by multiple linear regression using  $\mathbf{X} \times \mathbf{a} = \mathbf{b}$ , where  $\mathbf{X}$  is the  $n \times p$  matrix of scaled inputs and  $\mathbf{b}$  is the vector of  $n$  outputs from the  $n$  computational experiments. Each value in the vector  $\mathbf{a}$  is normalized to range from 0 to 1, where higher numbers indicate greater importance for the corresponding parameter in matrix  $\mathbf{X}$ .

The above procedure merits a number of comments and explanations. First, Table 5 shows the bounds of the various

inputs to be varied in the global sensitivity analysis. In general, the bounds on any given parameter are wider than necessary to capture the variation of a single experiment, which allows them to capture the range of uncertainty seen in the body of char combustion research. Specific details are given where needed in the table. Also, the kinetic parameters are not shown, as they were initially determined to be highly sensitive parameters and then fixed at optimized values for all of the analyses shown in this work.

Also note that the system is solved by linear regression, implying that each parameter has a linear impact on char burnout and particle temperature. This is not entirely true, resulting in a degree of fitting error, but each parameter was checked by performing a series of model executions where only the parameter in question was adjusted over its range while all others remained at their nominal values. In these computations, a straight line reasonably approximated the vast majority of changes in output vs changes in input, and the exceptions were excluded from the analysis. Here, “reasonably” approximated by a line means that a linear fit was adequate to examine the sensitivity of the parameter but not necessarily adequate to precisely track changes in output induced by the change to the input in question. Those few cases that were not reasonably linear together with those that were unsuitable for partial rank correlation (see below) constituted roughly 5% of the data and were excluded from the analyses.

The multiple linear regression was used to solve eq 15 where  $\mathbf{X}$  is the  $n \times p$  matrix of parameter values,  $\mathbf{a}$  is the vector of importance measures for each of the  $p$  parameters, and  $\mathbf{b}$  is the vector of  $n$  outputs from the  $n$  computational experiments. The simplified case of a single computational experiment results in eq 16, where the more traditional output  $y$  replaces the vector  $\mathbf{b}$ . The partial derivative of  $y$  with respect to the  $i$ th parameter yields eq 17, which shows that the  $i$ th importance measure is the derivative of the output with respect to the  $i$ th parameter, or in other words the slope of the output in the direction of the  $i$ th parameter. On a normalized scale of inputs between  $-1$  and  $1$ , the importance measure is approximately a measure of how rapidly a change in the  $i$ th input induces a change in the output  $y$ , and because the rate is constant over a scaled parameter space, it is also a measure of the magnitude of the total change in output.

$$\mathbf{X} \times \mathbf{a} = \mathbf{b} \quad (15)$$

$$x_1 a_1 + x_2 a_2 + \dots + x_p a_p = y \quad (16)$$

$$\frac{\partial y}{\partial x_i} = a_i \quad (17)$$

In  $p$  dimensions (for the  $p$  parameters in the sensitivity analysis), eq 18 is the solution to eq 12 and is identical to setting the gradient of eq 19 equal to zero, or minimizing the sum-squared-of-error in all  $p$  dimensions (where the error is the residual between the actual CCK output and the linearized model prediction for the CCK output). The solution vector  $\mathbf{a}$  is therefore the best estimate of the importance measures in that it minimizes the difference between the regression predictions and the actual results of the model. The vector  $\mathbf{a}$  is analogous to the slope of the change in output related to the change in input but differs in that it captures some influence of the higher order effects of all other parameters (i.e.,  $\mathbf{a}_i$  is **not** the same as would be found by simply varying parameter  $i$  in isolation and finding the slope at the minimum and maximum of the allowed values

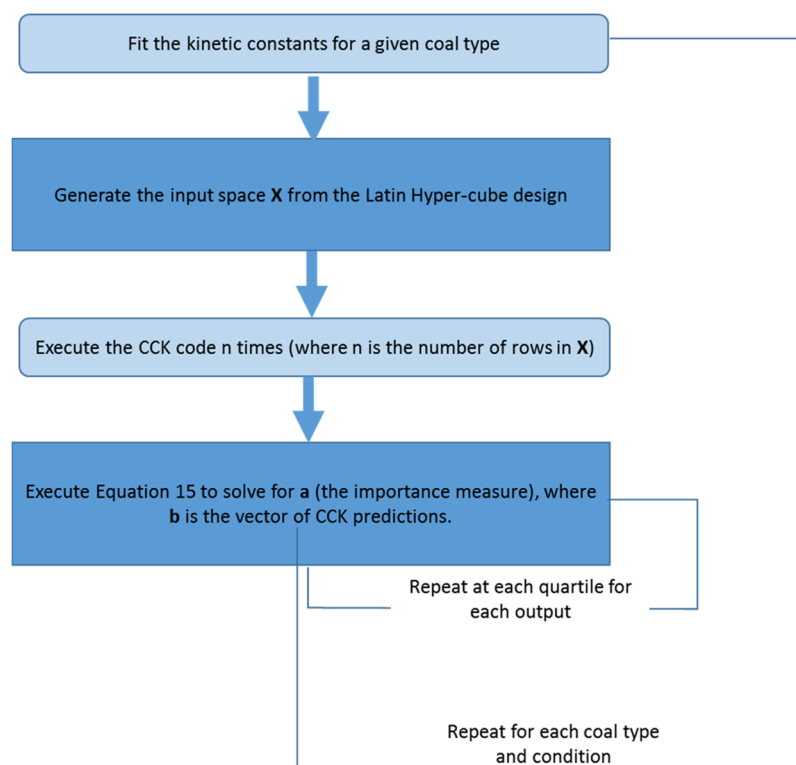


Figure 4. Logic diagram to find the sensitivity measure for a given output.

Table 6. Total Sensitivity Measures for All O<sub>2</sub> Conditions and Each Individual Condition

mean sensitivity measure		sensitivity					
		for $y_{O_2} = 0.12$		for $y_{O_2} = 0.24$		for $y_{O_2} = 0.36$	
variable	importance	variable	importance	variable	importance	variable	importance
$E_A$	0.74	$E_A$	0.76	$E_A$	0.72	$E_A$	0.75
$n_1$	0.51	$n_1$	0.55	$n_1$	0.51	$n_1$	0.48
$d/d_0$	0.27	$d/d_0$	0.40	$d/d_0$	0.22	$\alpha$	0.22
$\alpha$	0.20	$d_{\text{grain}}$	0.20	$\alpha$	0.22	$\sigma_{E^A}$	0.20
$d_{\text{grain}}$	0.20	$t_r$	0.18	$d_{\text{grain}}$	0.21	$d_{\text{grain}}$	0.19
$\sigma_{E^A}$	0.18	$\alpha$	0.18	$\sigma_{E^A}$	0.17	$d/d_0$	0.17
$t_r$	0.14	$\sigma_{E^A}$	0.17	$t_r$	0.12	$t_r$	0.11

of parameter  $i$ . Figure 4 is a block logic diagram of the sensitivity analysis process.

$$\mathbf{a} = (\mathbf{X}'\mathbf{X})^{-1}\mathbf{X}'\mathbf{b} \quad (18)$$

$$\text{SSE} = \sum_i r_i^2 = \sum_i (y_i - f(x_i, \mathbf{a}))^2 \quad (19)$$

**4.4. Partial Rank Correlation Coefficients.** Partial rank correlation coefficients (PRCC), or Spearman correlation coefficients, establish the degree of monotonic relation between outputs and inputs after taking into account the effects of other input parameters, with +1 indicating perfectly monotonic, positive correlation, while -1 indicates perfectly monotonic anticorrelation.<sup>20</sup> PRC coefficients were found in three steps. First, the residuals were found by solving a series of multiple linear regressions where eq 15 is solved repeatedly without one of the  $p$  columns (where each column contains values of one of the  $p$  parameters needed to execute the CCK code). This series of regressions results in a series of models, each missing one of the parameters. The difference between the predictions from the full model and the predictions from the model missing the

$i$ th parameter are the  $i$ th residuals, because they are the portion of the model that cannot be explained without the  $i$ th parameter. Second, after the residuals are calculated, they are ranked by assigning the number 1 to the lowest valued residual, the number 2 to the second lowest value, and so forth until  $n$  (the integer number of experiments) is assigned to the highest value. This step is also applied to the predicted output of interest,  $\mathbf{b}$  (burnout or particle temperature). The third and final step is to calculate the correlation coefficient for the residuals, as in eq 20.<sup>21</sup> This sensitivity measure captures nonlinear effects of the input parameters on the output, provided the effects are monotonic and the inputs have no significant correlation with each other. As mentioned above, the small fraction of the data that failed to meet these criteria was excluded from the analysis.

$$\rho_{X,Y} = \frac{\text{cov}(X, Y)}{\sigma_X \sigma_Y} \quad (20)$$

It is also worth noting that while the PRCC method is designed to rank the monotonic correlation of individual

Table 7. Mean Total Sensitivity for Particle Temperature, Burnout, PRCC, and Linear Approximation

sensitivity for particle burnout		sensitivity for particle temperature		sensitivity for PRC coefficients		sensitivity for linear approximation	
variable	importance	variable	importance	variable	importance	variable	importance
$E_A$	0.82	$E_A$	0.58	$E_A$	0.62	$E_A$	0.90
$n_1$	0.53	$n_1$	0.50	$n_1$	0.43	$n_1$	0.62
$d/d_0$	0.34	$d_{\text{grain}}$	0.31	$d/d_0$	0.26	$d/d_0$	0.28
$\sigma_{E^A}$	0.21	$\alpha$	0.29	$\alpha$	0.16	$d_{\text{grain}}$	0.26
$\alpha$	0.12	$d/d_0$	0.20	$d_{\text{grain}}$	0.15	$\alpha$	0.24
$t_r$	0.11	$t_r$	0.17	$\sigma_{E^A}$	0.13	$\sigma_{E^A}$	0.23
$d_{\text{grain}}$	0.08	$\sigma_{E^A}$	0.16	$t_r$	0.13	$t_r$	0.15

variables, it cannot perfectly discount the effects of other variables or the misfit of the full model. The high number of replicates helps to overcome this noise, but a parameter that induces a small change in outputs will probably not have as high a sensitivity ranking as a parameter that induces an exponential shift, even if the smaller change is more perfectly monotonic, because the small change is far more likely to be lost in the noise. The PRCC measure is therefore somewhat of a measure of the magnitude of the change induced in an output parameter.

## 5. RESULTS AND DISCUSSION

Simulations of four coals at each of three conditions for two different sensitivity tests of 27 parameters resulted in approximately 5,000 sensitivity measures, and a plethora of relevant comparisons. To make direct comparisons of all sensitivity measures, the linear approximation importance measures were normalized to range between 0 and 1, and the absolute value was taken of PRC coefficients, so they indicate only a magnitude of importance, not correlation or anticorrelation. Relevant subsets of the sensitivity analysis are discussed below.

### 5.1. Total Sensitivity at Various $O_2$ Concentrations.

Table 6 shows the total sensitivity scores (the mean of all sensitivity scores over all experiments and conditions) of the seven most important variables in the CCK code at all coals at all conditions, for all outputs, and for a combination of both PRCC and linear approximation tests. It also shows the total sensitivity for each of the three  $O_2$  levels tested.

The scores shown in the “importance” column are the mean scores for the seven most important variables as measured from all the various combinations of conditions and analysis techniques. Note that although residence time ( $t_r$ ) is not typically thought of as a model parameter, the quartile of residence time was included as a parameter in the sensitivity analysis codes to differentiate between sensitivity early in burnout and late in burnout. Residence time, along with the other six parameters shown in Table 6, are also the most sensitive in each individual analysis (with a minor exception discussed below). The same two variables are always of highest importance and always have the same relative position: mean annealing activation energy ( $E_A$ ) and the order of the oxidation reaction ( $n_1$ ). As such, these two parameters will be referred to as having primary importance, while the other five variables will be referred to as secondary, and the remaining 20 are considered to have tertiary importance. Though the seven most sensitive variables are the same in all analyses, and they share many common trends in sensitivity scores from one analysis to the next, there are several interesting differences in each group of analyses.

In the case of the analyses of each  $O_2$  mole fraction shown in Table 6, the particle swelling/raw coal initial diameter ( $d/d_0$ ) becomes less important as  $O_2$  concentration increases. The swelling and initial diameter parameters were lumped together because they are so closely linked in the CCK code, and in all other cases they parallel each other quite closely, but in the case of varying  $O_2$  concentration the decreased importance of  $d/d_0$  is largely due to the decreased impact of the initial particle diameter. This decreased importance is due to higher  $O_2$  concentrations rapidly (too rapidly to be realistic in fact) consuming the bulk of the carbon, leaving an ash-rich char particle with less variability in particle size for most of the residence time. Similarly, the importance of residence time steadily decreases with  $O_2$  concentration because the carbon is converted quite quickly at high- $O_2$  levels, so late-stage burnout has progressively less variability.

### 5.2. Sensitivity for All Coal Types and All Combustion

**Conditions.** The subset of the sensitivity analyses for all coal types and combustion conditions are shown in Table 7, including the mean scores for sensitivity to particle temperature and burnout (averaged between PRCC and linear approximation tests), and the breakdown for the PRCC and linear approximation sensitivity tests (averaged between sensitivities for both burnout and particle temperature). The two outputs (burnout and particle temperature) are most sensitive to the same seven variables but differ somewhat in the ordering of those variables. Note that the particle temperature predictions are considerably less sensitive than burnout predictions to  $E_A$  and  $d/d_0$ . The annealing parameters are likely more important in burnout because the kinetics they control determine how quickly the particle reaches low reactivity in late-stage burnout, but the relatively reactive particle in early burnout is both heated by initially rapid combustion and cooled by relatively high gasification rates, lessening the effects of high reactivity on particle temperature. Similarly,  $d/d_0$  affects the surface area available, but while this affects burnout substantially, the combination of endothermic and exothermic reactions again lessens the reactivity effects on particle temperature. On the other hand, the mode of burning parameter ( $\alpha$ ) is approximately 250% more important in particle temperature prediction than the burnout prediction, and the ash grain diameter is nearly four times more important. This is because  $\alpha$  is indicative of the combustion regime (zone I, II, or III), which is fixed in the model for the entire system, but potentially different between the endothermic and exothermic reactions, and ash grain diameter ( $d_{\text{grain}}$ ) is most important in late-stage burnout as the ash film model reduces reaction rates and allows other system parameters to significantly affect the temperature, while burnout is nearly complete in that region and not as heavily impacted.

**5.3. Subbituminous vs High-Volatile Bituminous Coals.** Comprehensive char combustion codes should ideally function for all coal types, so it is particularly relevant to compare the prediction sensitivity for multiple coals and coal types. The data were for two high-volatile bituminous and two subbituminous coals, and Table 8 compares their total

**Table 8. Mean Total Sensitivity for Particle Temperature and Burnout Using Either the PRCC or Linear Approximation Method for Different Coal Types**

variable	importance					
	subbituminous			bituminous		
	total	PRCC	linear approx	total	PRCC	linear approx
$E_A$	0.72	0.66	0.89	0.76	0.58	0.99
$n_1$	0.67	0.56	0.82	0.4	0.31	0.50
$d/d_0$	0.24	0.24	0.24	0.29	0.27	0.31
$\alpha$	0.21	0.16	0.26	0.2	0.16	0.24
$d_{\text{grain}}$	0.20	0.15	0.27	0.2	0.14	0.25
$\sigma_{E_A}$	0.17	0.15	0.19	0.19	0.12	0.26
$t_r$	0.13	0.12	0.14	0.14	0.13	0.16

importance measures and the breakdown between PRCC and the linear approximation. The total importance is an average between the PRCC and linear approximation methods, weighted by the number of importance measures in each.

The subbituminous and high-volatile bituminous coals are striking in how closely they parallel each other in each of the three breakdowns above, with one exception. The subbituminous coal exhibits much higher sensitivity to the order of the oxidation reaction than the high-volatile bituminous coals, probably because the subbituminous coal is more reactive and oxidation is the dominant conversion reaction. Note that, in the CCK code, oxidation is governed by a Langmuir–Hinshelwood-type reaction in which  $n_1$  is the reaction order of one of the three reactions that constitute the oxidation reaction expression. Coal conversion data suggest that  $n_1$  should be between 0 and 1, with the value depending on the reaction temperature. In a global reaction expression, the value of  $n_1$  would change according to the combustion regime, while, in the CCK code, the Langmuir–Hinshelwood expression adjusts the weight of the term containing  $n_1$  depending on conditions to appropriately capture the change in apparent order.<sup>8,22</sup>

Table 8 also highlights a difference between the PRCC and linear approximations also seen in Table 7; the linear approximation generally gives markedly higher sensitivity measures than the PRCC method. This is not unexpected since the two sensitivity tests do not measure the same thing, so they should not have exactly the same sensitivity. The linear

approximation test is reporting the rate that the outputs change due to a change in a given input, while the PRCC method is reporting the degree of monotonic behavior in the change induced in an output by a change in input and also indicates the rough magnitude of that change (because small changes are likely to get lost in the noise). The two methods together give a more complete view of the model and here indicate that the rate of change is generally slightly greater than the monotonicity of the change.

**5.4. Sensitivity at Quartiles of Residence Time.** The life of a coal particle in an oxy-coal system includes a period of heating/devolatilization, rapid initial reaction, potential additional heating or cooling depending on relative concentrations of reactive gases, and late-stage burnout. It is reasonable to expect different model parameters to be important at different burnout stages, so Table 9 summarizes the model sensitivity at each quartile of residence time.

The sensitivity scores in Table 9 show a slight trend for model sensitivity to  $n_1$  to decrease at later quartiles, which, as alluded to above, is unsurprising since most of the carbon has been consumed as burnout progresses, giving other model parameters relatively greater importance. The residence time on the other hand shows the opposite trend;  $t_r$  becomes more and more important at later quartiles. Most striking, however, is the change induced by particle swelling. The sensitivity to  $d/d_0$  is quite large for the first and second quartiles but less important in late stages of burnout, which also is to be expected since the bulk of the carbon is eaten away at high  $t_r$ , leaving an ash-rich particle. Note that the first quartile included a minor exception to the sensitivity trends and showed that the  $O_2$  concentration (which was allowed to vary up to 10% of the total  $O_2$  mole fraction) had a sensitivity measure of 0.12, displacing  $t_r$  from the list of most important variables. However, the importance value for  $t_r$  in the first quartile was left in the table for comparative purposes.

**5.5. Additional Discussion.** The most influential parameters are discussed below.

**5.5.1. Thermal Annealing.** Both thermal annealing sub-model parameters are in the top seven parameters, and the mean activation energy is consistently the most sensitive variable. Also, the annealing submodel currently in use is extremely rapid and does not distinguish between active sites, despite evidence that the active complex for each of the three main carbon conversion paths is distinct.<sup>9,10</sup> The initial rapid pace of the annealing submodel is not necessarily problematic, since it is a result of a somewhat unrealistic distributed activation energy. The most advanced annealing submodels use a distribution of activation energies to capture the numerous reactions involved in thermal annealing, and these submodels are largely reconcilable with each other,<sup>23</sup> but they include

**Table 9. Sensitivity Scores by Quartile of Residence Time**

quartile 1		quartile 2		quartile 3		quartile 4	
variable	importance	variable	importance	variable	importance	variable	importance
$E_A$	0.73	$E_A$	0.72	$E_A$	0.77	$E_A$	0.76
$n_1$	0.59	$n_1$	0.52	$n_1$	0.48	$n_1$	0.46
$d/d_0$	0.40	$d/d_0$	0.29	$\alpha$	0.23	$\alpha$	0.22
$d_{\text{grain}}$	0.18	$\alpha$	0.21	$d_{\text{grain}}$	0.21	$d_{\text{grain}}$	0.21
$\alpha$	0.16	$d_{\text{grain}}$	0.20	$\sigma_{E_A}$	0.20	$\sigma_{E_A}$	0.20
$\sigma_{E_A}$	0.15	$\sigma_{E_A}$	0.19	$d/d_0$	0.19	$t_r$	0.19
$t_r$	0.10	$t_r$	0.11	$t_r$	0.15	$d/d_0$	0.18

unrealistic tails in the distribution. In the case of the activation energy employed in CBK and its offshoots, the log-normal distribution has a portion of annealing reactions with such low activation energies that they occur instantaneously. This problem could be solved by truncating the distribution, but there is no clear-cut truncation point, and since the distribution is consistent, it does not invalidate the model as a whole, as long as the gasification preexponential factors are calibrated in conjunction with the annealing parameters.

However, the same submodel has appeared in successive models without necessarily accounting for the relation between initial preexponential factors and annealing model parameters. The particular annealing model in CBK and its successors is presented by Hurt et al.<sup>10</sup> as formulated by Suuberg,<sup>24</sup> and, contrary to the enormous impact seen in the sensitivity analysis, past experience has shown relatively small influence due to annealing, especially in late burnout.<sup>12,25</sup> Furthermore, the current annealing model fails to account for the dominant effects of peak particle temperature, particle heating rate, and coal precursor. These preparation conditions and differences in coal chemistry radically change the annealing activation energy distribution,<sup>25,26</sup> but the prior model has no method to incorporate this information and was developed prior to sufficient available data to reasonably predict changes in the reaction pathway based on preparation conditions. It is likely that an entirely new annealing model is needed so that char annealing occurs along a more realistic path and distinguishes between gasification and oxidation reactive sites.

**5.5.2. Reaction Order.** The global oxidation reaction order ( $n_1$ ) likely changes depending on the temperature regime, but should lie between 0 and 1.<sup>7,8</sup> The three-step oxidation model can switch between the different reaction orders at various temperatures, so despite the sensitivity of this parameter, it is appropriate in the current Langmuir–Hinshelwood-type kinetic scheme.

**5.5.3. Residence Time.** The residence time, while important, is experimentally measured or an input from the simulation and does not rely on submodels, so it should of course be carefully measured, but does not impact the model construction. It was explored as a sensitive parameter only to observe how important uncertainty in residence time might be. Given that char burnout experiments tend to have relatively low burnout and short residence times (except in TGA systems), the high sensitivity of this parameter to small changes is worth noting.

**5.5.4. Ash Inhibition.** The ash inhibition submodel originally outlined by Hurt et al.<sup>10</sup> is currently used in the CBK offshoots and depends on  $d_{\text{grain}}$ . This submodel relies on building on ash film, which immediately begins to reduce the combustion rate. However, a more sophisticated model developed by Niu and Shaddix<sup>27</sup> allows ash to build a film and to diffuse back into the carbon core and effectively dilute the carbon in later stages of burnout. This model may be more realistic and may better explain late-stage burnout data.

**5.5.5. Mode of Burning.** The mode of burning parameter describes the changes in diameter and density and is related to combustion regime. Currently, the model uses only one regime for all reactions and the entire computation, which gives contradictory results for either gasification or oxidation occurring simultaneously.  $\alpha$  is very commonly used in carbonaceous particle combustion models to describe the shrinking particle and decreasing particle density, but the value of  $\alpha$  is given as a constant throughout burnout. Haugen et al.,<sup>28</sup> developed a much more realistic model that uses the

effectiveness factor to appropriately weight mass loss between the particle exterior surface and the interior surface (diameter vs density change). All combustion models that have sufficient detail to capture changing particle size and density would be improved by similarly allowing that change to depend on the effectiveness factor, which varies throughout burnout. In the case of oxy-coal, this modification is especially impactful because  $\text{CO}_2$  and  $\text{H}_2\text{O}$  reactions are more important than in conventional air-fired coal combustion, and gasification reactions have very different effectiveness factors than the oxidation reaction.

**5.5.6. Particle Swelling.** The swelling and initial diameter require a better swelling model, such as the model developed by Shurtz et al.<sup>29</sup> to allow for high heating rates and pressure. Currently the swelling model in the CCK code is quite crude and does not adequately account for radical changes in swelling with coal type and char preparation conditions. Also, any comprehensive combustion model is likely to be too expensive to directly include in a CFD model, so the swelling model will likely be used to train global models to the specific conditions in question. Because pulverized coal has a distribution of particle sizes, the training code should be run for a series of size bins, sufficiently refined so that particle size is no longer a significant source of uncertainty in the trained global model.

## 6. CONCLUSIONS AND RECOMMENDATIONS

A sensitivity analysis of an advanced char conversion model (CCK) was performed based on data for two subbituminous and two high-volatile bituminous coals in an oxy-coal environment. The results were analyzed using a linear approximation sensitivity analysis method and the partial rank correlation coefficients method. These analyses revealed the expected importance of kinetic parameters. However, after the kinetic values were found from an optimized fit with data, the subsequent set of analyses found that the two most important parameters were the activation energy of char annealing ( $E_A$ ) and a reaction order ( $n_1$ ). Five other parameters were found to be of secondary importance: initial char diameter ( $d/d_0$ ), ash grain size ( $d_{\text{grain}}$ ), distribution of the activation energy for annealing ( $\sigma_{E_A}$ ), the quartile of residence time ( $t_r$ ) distinguishing early burning behavior from late burning behavior, and the mode of burning parameter ( $\alpha$ ) which controls diameter and density change. These seven variables are prime candidates for future research to improve the accuracy and predictive power of the CCK char conversion code (and comprehensive char codes in general). These results imply a need to carefully quantify and minimize the uncertainty in the seven most sensitive variables.

## ■ AUTHOR INFORMATION

### Corresponding Author

\*E-mail: [tom\\_fletcher@byu.edu](mailto:tom_fletcher@byu.edu). Tel.: 1-801-422-6236.

### Notes

Disclosure: This publication was prepared as an account of work sponsored by an agency of the United States Government. Neither the United States Government nor any agency thereof, nor any of their employees, makes any warranty, express or implied, or assumes any legal liability or responsibility for the accuracy, completeness, or usefulness of any information, apparatus, product, or process disclosed, or represents that its use would not infringe privately owned rights. Reference herein to any specific commercial product, process, or service by trade name, trademark, manufacturer, or

otherwise does not necessarily constitute or imply its endorsement, recommendation, or favoring by the United States Government or any agency thereof. The views and opinions of authors expressed herein do not necessarily state or reflect those of the United States Government or any agency thereof.

The authors declare no competing financial interest.

## ACKNOWLEDGMENTS

This material is based upon work supported by the Department of Energy, National Nuclear Security Administration, under Award No. DE-NA0002375. Funding for this work was also provided by the Department of Energy through the Carbon Capture Simulation Initiative.

## REFERENCES

- (1) Wall, T.; Liu, Y. H.; Spero, C.; Elliott, L.; Khare, S.; Rathnam, R.; Zeenathal, F.; Moghtaderi, B.; Buhre, B.; Sheng, C. D.; Gupta, R.; Yamada, T.; Makino, K.; Yu, J. L. An Overview on Oxyfuel Coal Combustion-State of the Art Research and Technology Development. *Chemical Engineering Research & Design* **2009**, *87* (8A), 1003–1016.
- (2) Scheffknecht, G.; Al-Makhadmeh, L.; Schnell, U.; Maier, J. Oxy-Fuel Coal Combustion—a Review of the Current State-of-the-Art. *Int. J. Greenhouse Gas Control* **2011**, *5*, S16–S35.
- (3) Hecht, E. S.; Shaddix, C. R.; Geier, M.; Molina, A.; Haynes, B. S. Effect of CO<sub>2</sub> and Steam Gasification Reactions on the Oxy-Combustion of Pulverized Coal Char. *Combust. Flame* **2012**, *159*, 3437–3447.
- (4) Shurtz, R. C. Effects of Pressure on the Properties of Coal Char under Gasification Conditions at High Initial Heating Rates. Ph.D. Dissertation; Chemical Engineering, Brigham Young University, Provo, UT, USA, 2011.
- (5) Shurtz, R. C.; Fletcher, T. H. Coal Char-CO<sub>2</sub> Gasification Measurements and Modeling in a Pressurized Flat-Flame Burner. *Energy Fuels* **2013**, *27*, 3022–3038.
- (6) Shaddix, C. R.; Molina, A. Particle Imaging of Ignition and Devolatilization of Pulverized Coal During Oxy-Fuel Combustion. *Proc. Combust. Inst.* **2009**, *32*, 2091–2098.
- (7) Geier, M.; Shaddix, C. R.; Davis, K. A.; Shim, H. S. On the Use of Single-Film Models to Describe the Oxy-Fuel Combustion of Pulverized Coal Char. *Appl. Energy* **2012**, *93*, 675–679.
- (8) Niksa, S.; Liu, G. S.; Hurt, R. H. Coal Conversion Submodels for Design Applications at Elevated Pressures. Part I. Devolatilization and Char Oxidation. *Prog. Energy Combust. Sci.* **2003**, *29*, 425–477.
- (9) Liu, G. S.; Niksa, S. Coal Conversion Submodels for Design Applications at Elevated Pressures. Part II. Char Gasification. *Prog. Energy Combust. Sci.* **2004**, *30*, 679–717.
- (10) Hurt, R.; Sun, J. K.; Lunden, M. A Kinetic Model of Carbon Burnout in Pulverized Coal Combustion. *Combust. Flame* **1998**, *113*, 181–197.
- (11) Bhatia, S. K.; Perlmutter, D. D. A Random Pore Model for Fluid-Solid Reactions. 2. Diffusion and Transport Effects. *AIChE J.* **1981**, *27* (2), 247–254.
- (12) Sun, J. K.; Hurt, R. H. Mechanisms of Extinction and near-Extinction in Pulverized Solid Fuel Combustion. *Proc. Combust. Inst.* **2000**, *28*, 2205–2213.
- (13) Lewis, A. D.; Holland, T. M.; Marchant, N. R.; Fletcher, E. G.; Henley, D. J.; Fuller, E. G.; Fletcher, T. H. Steam Gasification Rates of Three Bituminous Coal Chars in an Entrained-Flow Reactor at Pressurized Conditions. *Energy Fuels* **2015**, *29*, 1479–1493.
- (14) McKay, M. D.; Beckman, R. J.; Conover, W. J. Comparison of Three Methods for Selecting Values of Input Variables in the Analysis of Output from a Computer Code. *Technometrics* **1979**, *21* (2), 239–245.
- (15) Frenklach, M.; Packard, A.; Feeley, R. *Modeling of Chemical Reactions*; Elsevier Science: Amsterdam, The Netherlands, 2005; Vol. 42, p 316.
- (16) Box, G.; Draper, N. *Empirical Model-Building and Response Surfaces*; John Wiley & Sons: New York, NY, USA, 1987; p 604.
- (17) Saltelli, A.; Ratto, M.; Andres, T.; Campolongo, F.; Cariboni, J.; Gatelli, D.; Saisana, M.; Tarantola, S. *Global Sensitivity Analysis: The Primer*; John Wiley & Sons: Hoboken, NJ, USA, 2008; p 304.
- (18) Saltelli, A.; Tarantola, S.; Campolongo, F.; Ratto, M. *Sensitivity Analysis in Practice: A Guide to Assessing Scientific Models*. Wiley: 2004; p 232.
- (19) Bhatia, S. K.; Perlmutter, D. D. A Random Pore Model for Fluid-Solid Reactions. 2. Diffusion and Transport Effects. *AIChE J.* **1981**, *27* (2), 247–254.
- (20) Gomero, B. Latin Hypercube Sampling and Partial Rank Correlation Coefficient Analysis Applied to an Optimal Control Problem. Masters, Mathematics, University of Tennessee, Knoxville, TN, USA, 2012.
- (21) Marino, S.; Hogue, I. B.; Ray, C. J.; Kirschner, D. E. A Methodology for Performing Global Uncertainty and Sensitivity Analysis in Systems Biology. *J. Theor. Biol.* **2008**, *254* (1), 178–196.
- (22) Hurt, R. H.; Calo, J. M. Semi-Global Intrinsic Kinetics for Char Combustion Modeling. *Combust. Flame* **2001**, *125* (3), 1138–1149.
- (23) Senneca, O.; Salatino, P. Loss of Gasification Reactivity toward O<sub>2</sub> and CO<sub>2</sub> Upon Heat Treatment of Carbons. *Proc. Combust. Inst.* **2002**, *29*, 485–493.
- (24) Suuberg, E. M., Thermally Induced Changes in Reactivity of Carbons. In *Fundamental Issues in Control of Carbon Gasification Reactivity*, Ehrburger, P., Lahaye, J., Eds.; Kluwer Academic: Dordrecht, The Netherlands, 1991; pp 269–299.
- (25) Shim, H. S.; Hurt, R. H. Thermal Annealing of Chars from Diverse Organic Precursors under Combustion-Like Conditions. *Energy Fuels* **2000**, *14* (2), 340–348.
- (26) Senneca, O.; Salatino, P. Overlapping of Heterogeneous and Purely Thermally Activated Solid-State Processes in the Combustion of a Bituminous Coal. *Combust. Flame* **2006**, *144* (3), 578–591.
- (27) Niu, Y. Q.; Shaddix, C. R. A Sophisticated Model to Predict Ash Inhibition During Combustion of Pulverized Char Particles. *Proc. Combust. Inst.* **2015**, *35*, 561–569.
- (28) Haugen, N. E. L.; Tilghman, M. B.; Mitchell, R. E. The Conversion Mode of a Porous Carbon Particle During Oxidation and Gasification. *Combust. Flame* **2014**, *161* (2), 612–619.
- (29) Shurtz, R. C.; Hogge, J. W.; Fowers, K. C.; Sorensen, G. S.; Fletcher, T. H. Coal Swelling Model for Pressurized High Particle Heating Rate Pyrolysis Applications. *Energy Fuels* **2012**, *26* (6), 3612–3627.